12th CIRP Conference on
Photonic Technologies [LANE 2022]

Industrial Paper

In-line Analysis of the Influence of Copper Pin-Pair Position on Laser Welding Process Results with Optical Coherence Tomography

Thomas Will[a,b,c,*], Johannes Müller[d], Ricus Müller[d], Claudio Hölbling[c], Christian Goth[c], Michael Schmidt[a,b]

[a]*Institute of Photonic Technologies, Friedrich-Alexander Universität Erlangen-Nürnberg, Konrad-Zuse-Straße 3/5, 91052 Erlangen, Germany*
[b]*Erlangen Graduate School in Advanced Optical Technologies (SAOT), Friedrich-Alexander Universität, 91052 Erlangen, Germany*
[c]*Vitesco Technologies Germany GmbH, Sieboldstraße 19, 90411 Nürnberg, Germany*
[d]*Vitesco Technologies Germany GmbH, Sickingenstraße 42-46, 10553 Berlin, Germany*

* Corresponding author. Tel.: +49 9131 85-23236; *E-mail address:* thomas.will@lpt.uni-erlangen.de

Abstract

Laser welding of copper hairpins gains importance for the automotive industry. The hairpins might be misaligned due to previous manufacturing steps. The misalignment leads to poor weld connections with reduced electrical conductivity. Optical coherence tomography (OCT) enables pre-process observation of the hairpin alignment as well as post-process observation of the welding result by inline scanning the weld topography. In this work, a proof-of-concept is demonstrated for welding result categorization of copper pin-pairs from post-process OCT data. A quantified separation of process results is possible which allows for concluding on misalignments in the pin-pair position.

Keywords: laser welding, optical coherence tomography, OCT, process monitoring, hairpin technology

1. Introduction

The electric engine is one of the most important components of the electrified powertrain. An efficient hairpin wound stator requires copper wires in the form of rectangular copper hairpins. Laser welding is applied to produce a conductive connection between these hairpins. The manufacture of stators includes several process steps before producing a conductive connection between hairpins. One of these process steps is the twisting process, where the copper wires are bent into pin pairs before being contacted with each other by laser welding [1]. After the twisting process, the hairpins might be misaligned, but the relative offsets are not monitored as an input variable. A singular poor weld connection may lead to scrap. A scrap of 1000 ppm in annual production of 1 000 000 pieces results in annual costs of 100 000 € considering a stator price of 100 €. Hence, the reduction of scrap by identifying defective welds with an inline monitoring technology may amortize the costs for the system technology within a year.

Optical coherence tomography (OCT) is an interferometric process monitoring technology, that enables inline quality control of the weld bead by non-destructive distance measurement [2-6]. OCT can be applied to identify misalignments in pre-process monitoring and the shape of the resulting weld in the post-process monitoring stage [7, 8]. Baader et al. (2021) identified the potential of OCT for post-process characterization of welded hairpins, where a misalignment results in deformed surface topography of the weld shape. The deformed shape can be an indicator for a reduced connection area of the joint partners and hence a defective weld. However, the current state-of-art lacks quality-relevant features for the identification of misalignment-based weld results from OCT data.

In this work, we show a possibility for classifying good reference process results from bad misaligned process results based on surface topographical OCT data. For this reason, we performed experimental work by laser welding hairpins with different misalignment types and observed the resulting weld surface topography with inline

OCT measurement. Afterward, we identify a relevant feature for the description of the welding result based on the misalignment type.

2. Experimental methods

The experimental setup for hairpin welding consists of a programmable scanning optic with cross-jet, processing fiber-coupled laser, and OCT (see Fig. 1). The laser welding process is performed using a continuous wave disk laser (Trumpf TruDisk 8001) at a wavelength of 1030 nm with a maximum average power of 8 kW. The laser light is coupled into programmable focusing optics (Trumpf PFO 33-2) from a fiber with a core diameter of 100 µm. The focusing optic with an F-theta lens has a focal length of 345 mm and results in a laser spot diameter of 228 µm. The programmable optics use galvanometer scanners, that allow for scanning in an elliptical field of 240 × 140 mm^2. The OCT (Lessmüller OCT) is attached to the programmable focusing optics and enables a coaxial positioning of the measurement beam. The OCT is an SD-OCT with a superluminescent diode with a wavelength range from 820 nm to 860 nm. The measurement beam is detected by a spectrometer consisting of a 2048-pixel line sensor with a maximum measurement frequency of 70 kHz. The scanning OCT system has an axial resolution of 11 µm, while the lateral resolution in the measurement direction is 24 µm.

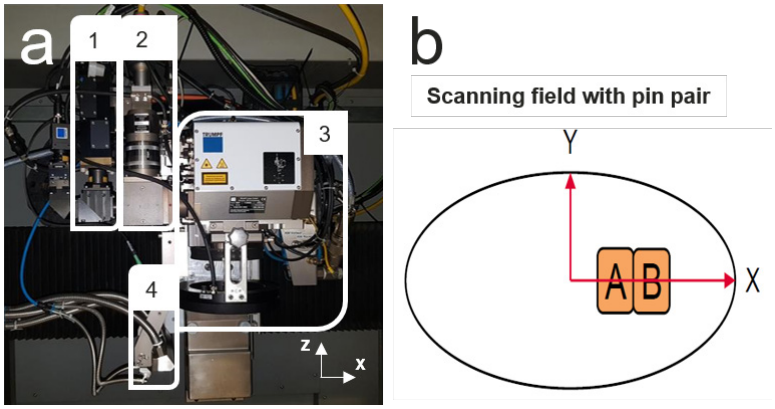

Fig. 1. Experimental setup (a) consisting of process monitoring technologies like OCT (1) as well as processing laser equipment like the laser fiber (2), programmable focusing optic (3), and cross-jet (4). Position of pin pair A and B in the scanning field of the programmable focusing optic for welding process (b).

Laser welding experiments are performed with pure copper hairpins (Cu-ETP) in the focus position. Two I-pins are welded in a clamping device within a welding area of 6.3 × 4.5 mm^2. The welding trajectory is constant with circular movements around the I-pins. The feed speed is between 12 m/min and 48 m/min at an average laser power between 3.7 kW and 6.0 kW. The investigated misalignment distances were varied by the misalignment type. Three types of misalignment are differentiated: axial misalignment (height difference in processing laser direction), lateral misalignment (relative misalignment between pins lateral to processing laser direction), and radial misalignment (gap between pin pair) (see Fig. 2). The lower limit of each misalignment type describes a reference measurement under ideal conditions. The offset for each misalignment type is increased with maximal increments of 0.4 mm until the upper limits are reached. The upper limits of each misalignment type (axial: 4.0 mm, lateral: 1.6 mm, radial: 1.0 mm) are chosen as very high values resulting either in no weld contact or no relevance in the practical application. Measurements are repeated five times for each set of parameters.

Three OCT measurement lines are used for inline scanning the weld topography. One is positioned centrally (y_0), whereas the other two measurement lines are at a distance of approximately 1.2 mm above/below the central measurement line (y_1/y_2). Each OCT measurement line is generated by the OCT scanner and has a length of 10 mm with 1000 measurement points.

As the resulting height profile from measurement line y_1 showed best results for the separation of misalignment types, features are only calculated for measurement results from this measurement line. We identified the linear trend t of the height profile as a relevant feature. Our selected feature calculates the least-squares regression line for the measurement points, which in turn can be described by attributes such as the slope or, in this case, the Pearson correlation coefficient. The correlation coefficient is a dimensionless measure of the degree of linear correlation between the height in measurement direction and the measurement position along the measurement line (here: linear trend). A value of either +1 or -1 indicates a completely positive (or negative) linear correlation between the characteristics under consideration.

In the following, examples of different pin-pair surface topographies are shown for the introduced misalignment types and the ability of the identified feature is discussed for the classification of hairpin welding results in good reference welds and bad misaligned welds.

3. Results and discussion

First, a qualitative distinguishability of the offset categories is discussed based on images from the central measurement position.

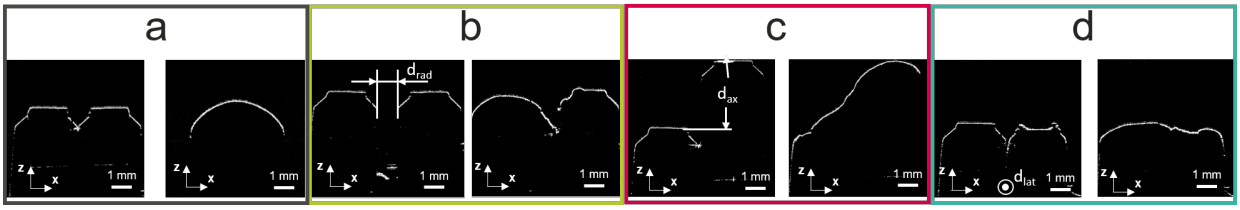

Fig. 2. OCT images for (a) reference measurement, (b) radial misalignment with an offset of 1.0 mm; (c) axial misalignment with an offset of 4.0 mm; (d) lateral misalignment with an offset of 1.6 mm. Each figure section shows a measurement before the welding process (left) and after the welding process (right).

Fig. 2 shows OCT images before and after the welding process for a reference measurement (a), radial (b), axial (c) and lateral (d) misalignment. Before the welding process, the surface topography of the rectangular pin pair can be seen with its chamfers. A smoothening of the measurement line contains the information of molten material after the welding process.

Fig. 2(a) shows a reference weld with no misalignment. The resulting weld bead shows a uniform round weld pearl and a homogeneous weld connection. Fig. 2(b) shows the gap between both joint partners in the case of a radial misalignment. The weld bead is non-uniform. The material of the non-offset left pin is more molten than that of the right pin. The outer contour of the right pin remains almost intact. The surface topography shows a bulge between the two pins as molten material can flow into the gap. Fig. 2(c) shows the axial height offset between both joint partners in the case of axial misalignment. Both joint partners were molten, but the resulting weld bead is skewed towards the lower joint partner. Fig. 2(d) shows a lateral offset between both joint partners. This offset is visible due to the irregular joint surface of the right pin, as the surface of the right pin is measured at its edge. The resulting weld bead shows a relatively flat weld bead.

A reference weld without misalignment shows a uniform round weld pearl on top of the hairpin ends and hence shows a symmetrical weld bead in contrast to either flat or skewed weld beads (compare Fig. 2). This difference in the surface topographical shape should allow for a good separability of good reference welds from bad misaligned welds based on the surface topography.

Fig. 3 shows the linear trend *t* for reference welds, axial, radial, and lateral misalignment.

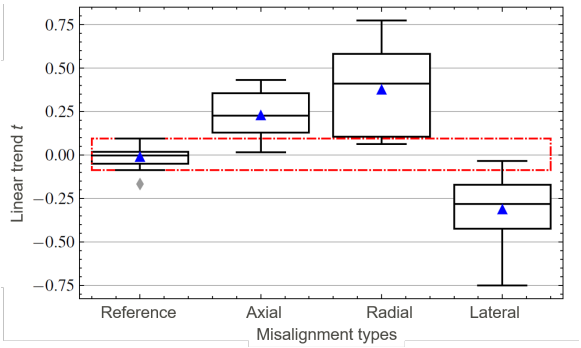

Fig. 3. Boxplot of the linear trend *t* as a function of the misalignment types. The arithmetic mean is indicated by a blue triangle. The ranges of the upper and lower quartiles of the reference are projected onto the remaining boxplots with a red box. Minimum and maximum values are indicated for each misalignment type. Outliers are marked as grey rhombus.

The arithmetic mean of the reference weld is 0 due to the symmetrical round shape of the weld pearl. The linear trend *t* increases depending on the left-/right-skewness of the weld bead towards positive/negative values. The skewed surface of the axial, radial, and lateral misalignment leads to a separability of the round reference weld from all other misalignment types (see Fig. 3). A differentiation between specific misalignment types like radial and axial misalignment is not possible by this feature. Feature values in the order of the reference weld can be also found for minima/maxima of other misalignment types (see Fig. 3, red box). These measurements in the overlap region can be assumed for small misalignments which lead to a rather symmetrical round reference surface topography.

4. Conclusion

In conclusion, a separation of process results is possible with the linear trend of the height profile. This feature supports the identification of poor weld connections by enabling a separation of symmetrical round reference welds from weld results with misalignments in the pin-pair position. Future surface topographical monitoring devices can apply this feature for an inline quality assessment of hairpin connections.

Acknowledgements

The authors gratefully acknowledge funding of the Erlangen Graduate School in Advanced Optical Technologies (SAOT) by the Bavarian State Ministry for Science and Art.

References

[1] T. Glaessel *et al.*, "Process Reliable Laser Welding of Hairpin Windings for Automotive Traction Drives," in *2019 International Conference on Engineering, Science, and Industrial Applications (ICESI)*, 2019: IEEE, pp. 1-6.

[2] C. Stadter, M. Schmoeller, M. Zeitler, V. Tueretkan, U. Munzert, and M. F. Zaeh, "Process control and quality assurance in remote laser beam welding by optical coherence tomography," *Journal of Laser Applications,* vol. 31, no. 2, p. 022408, 2019.

[3] C. Stadter, M. Schmoeller, L. von Rhein, and M. F. Zaeh, "Real-time prediction of quality characteristics in laser beam welding using optical coherence tomography and machine learning," *Journal of Laser Applications,* vol. 32, no. 2, p. 022046, 2020.

[4] M. Schmoeller, C. Stadter, S. Liebl, and M. F. Zaeh, "Inline weld depth measurement for high brilliance laser beam sources using optical coherence tomography," *Journal of Laser Applications,* vol. 31, no. 2, p. 022409, 2019.

[5] M. Kogel-Hollacher, S. André, and T. Beck, "Low-coherence interferometry in laser processing: A new sensor approach heading for industrial applications," in *Interferometry XIX*, 2018, vol. 10749: International Society for Optics and Photonics, p. 1074912.

[6] J. Hartung, A. Jahn, M. Stambke, O. Wehner, R. Thieringer, and M. Heizmann, "Camera-based spatter detection in laser welding with a deep learning approach," in *Forum Bildverarbeitung 2020*, 2020: KIT Scientific Publishing, p. 317.

[7] M. Baader, A. Mayr, T. Raffin, J. Selzam, A. Kühl, and J. Franke, "Potentials of Optical Coherence Tomography for Process Monitoring in Laser Welding of Hairpin Windings," in *2021 11th International Electric Drives Production Conference (EDPC)*, 2021: IEEE, pp. 1-10.

[8] N. D. Dupriez and A. Denkl, "Advances of OCT Technology for Laser Beam Processing: Precision and quality during laser welding," *Laser Technik Journal,* vol. 14, no. 4, pp. 34-38, 2017.